# An Electromagnetic-Simulation based Investigation of the Dielectric Padding Approach for Head Imaging at 7 T

Andreas Rennings[1], Keran Wang[1], Le Chen[1], Friedrich Wetterling[2], and Daniel Erni[1]

[1]*General and Theoretical Electrical Engineering (ATE), University of Duisburg-Essen, Duisburg, NRW, Germany*, [2]*Faculty of Engineering, Trinity College, Dublin University, Dublin, Ireland*

INTRODUCTION and OBJECTIVES: The use of dielectric pads in high-field MRI can help to improve the |B1+| homogeneity and/or reduce the peak specific absorption rate (SAR) [1-4]. It is usually based on cushions or films with a high permittivity and low loss tangent, which are added between the radio-frequency (RF) coil and the body's surface. Up to now the approach has been evaluated numerically using full-wave simulation of homogeneous and inhomogeneous body models (e.g. from the virtual family, and empirically using MR images and corresponding recordings of B1+ maps. Here we investigate the underlying physics behind the dielectric padding approach based on a simple 2-D setup including a homogeneous 15-cm-diameter cylinder-phantom modeling the human head at 300 MHz. We investigate the best suited pad permittivities for head imaging at 7T via computationally-efficient electromagnetic (EM) simulations. The cross-sections (e.g. sagittal or coronal planes) exhibiting the best and worst case |B1+| homogeneity are determined. Finally, we deliver an explanation for the working principle of the dielectric padding approach.

MATERIALS and METHODS: The EM field problem was solved numerically by using the full-wave finite element method (FEM) solver COMSOL Multiphysics. The chosen geometric setup is shown in Fig. 1. It encompasses the phantom (15 cm diameter, $\varepsilon_{phan} = 45.3$ & $\sigma_{phan} = 0.87$ S/m as these are the parameters chosen to generally replicate the electric head tissue properties via liquids in phantom experiments, head tissue simulating liquid, short HTSL [5]) modeling the human head at 300 MHz, two dielectric pads (5 cm thickness, 90° sector angle) with varied permittivity, ε_{pad}, ranging from 1 to 100, the active sheet with an impressed surface current density driven in z-direction ($J_z(\alpha, t) = J_0 \exp(2\pi ft-\alpha)$, travelling wave in +α direction) modeling a birdcage fed in quadrature mode, and on the outer perimeter a perfect electric conductor (PEC) shielding the EM field. The advantage of this rather abstract geometry choice over conventional implementation is that while it perfectly models the behavior of a circularly polarized birdcage the computational complexity is reduced to two-dimensions. Hence, one simulation took less than 5 seconds to compute, allowing us to reduce the step width of the pad permittivity to $\Delta\varepsilon_{pad} = 1$, yielding smooth plots for the coefficient of variation (CoV). This figure of merit calculated by built-in MATLAB routines specifies the homogeneity of the |B1+| field. We evaluated it in the phantom, along cross-sectional lines (for α = const) exhibiting the best and the worst CoV (CoV_best, CoV_worst, cf. Fig. 2). Additionally, the corresponding angle of the best and worst CoV-line is determined and plotted as well a function of ε_{pad}. In Fig. 3 the magnitude of $B_{1+} = (B_x + j B_y)/2$ and the z-component of the displacement current density ($J_D = j\omega D = j\omega\varepsilon E = $ curl H, to indicate the influence of the high pad permittivity onto the magnetic vector field) is given.
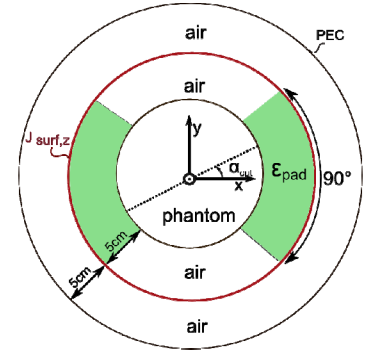

Fig. 1: 2-D setup modeling the EM-field generated by a circularly polarized birdcage incl. cylinder phantom, active sheet with impressed surface current, in the between the dielectric pads with varied permittivity, and a PEC shield.

RESULTS and DISCUSSION: In Fig. 2 CoV_best and CoV_worst inside the phantom are given as a function of ε_{pad}. The location of the cross-sectional-lines exhibiting the best and worst CoV in terms of their α-coordinate is shown as well (cf. also Fig. 3). We can distinguish the following regimes: For the first one, $\varepsilon_{pad} < 40$ ("lower"), CoV_best and CoV_worst are monotonically decreasing and increasing, respectively. For $40 < \varepsilon_{pad} < 70$ ("intermediate"), CoV_best is further reduced down to a CoV_min of 1%, whereas CoV_worst oscillates around a value of 60%; the final regime corresponds to $\varepsilon_{pad} > 70$ ("higher"), here CoV_best and CoV_worst increase both before these values start to vary quite strongly. For the first regime ("lower") the corresponding cross-sectional lines are located close to $\alpha_{best} = 135°$ and $\alpha_{worst} = 85°$, respectively, slightly rotating counter clockwise (CCW) with increasing ε_{pad}. Within the range, $40 < \varepsilon_{pad} < 45$, these cross-sectional-planes are rotating back (CW) to cross-sectional lines angled at 40° and 80°, respectively. Above an ε_{pad} of 60 both orientations (i.e. angles) increase again (CCW). Physically the three regimes can be explained by the number of extrema of the displacement current density (DCD, $j\omega D_z$) inside the pads. From visual inspection of the 2D results (cf. right column of Fig. 3) we observed that for the "lower" permittivity regime, e.g. $\varepsilon_{pad} = 10$, there is a broad "single-peak" DCD inside of each pad (top). For the intermediate permittivity range, e.g. $\varepsilon_{pad} = 50$, there are two peaks (bottom), and for the final regime there are even more DCD-extrema inside the pads. Such a DCD extrema comes along with a circulation of the magnetic vector field (bending of the corresponding field lines). With the pads we can remove the strong DCD extrema inside the phantom into the pads. Thus for the later case, the magnetic field is less "curly" inside the phantom and more "curly" inside the pads. Alternatively the phantom can be seen as a lossy dielectric resonator and the pads can be used to optimize its eigen-mode with a curl-less magnetic field distribution.

CONCLUSIONS: We presented a simple model and used it for EM simulations to get physical inside to the dielectric padding approach. We determined the best suited values for ε_{pad} and the cross-sectional-planes with best and worst CoV for the |B1+| profile.
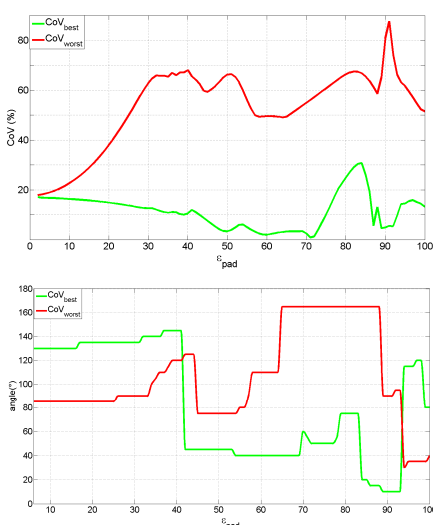
Fig. 2: Min. and max. CoV (top) as well as the corresponding angle of these cross-sectional lines (bottom), both as a function of ε_{pad}.
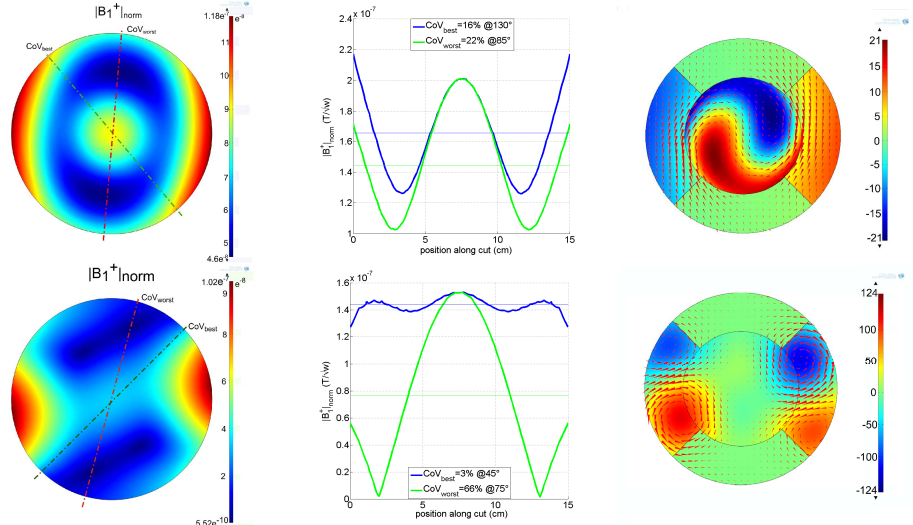
Fig. 3: |B1+| inside phantom (left), |B1+| along the cross-sectional lines with best and worst case CoV (middle) and displacement current together with magnetic vector field (right) for different pad permittivity: 10 (top row, with one-peak pattern in a pad), and 50 (bottom row, with two-peek pattern in a pad).

REFERENCES: [1] P. de Heer et al., Magn. Res. in Med.68:1317–1324 (2012) [2] Q. X. Yang et al., J Magn Reson Imag, 2006. [3] Z. Wang et al., Proc. ISMRM 20 (2010), no. 2701. [4] A. J. E. Raaijmakers et al., Magn. Reson. Med. (66), 2011. [5] A. Christ, et al., Phys Med Biol. (51), 2006.

M78NM&+5%"H FO#1E5+"4:&I%$, ε_{pad} $\in$ [1, 100]

Observations:

! cut-planes with improved |B1+|

! but also cut-planes with deteriorate |B1+| profile

! cut-planes with best & worst |B1+| profile ÒturnÓ with varied ε_{pad} $\in$ [1, 100]

$\boxed{\varepsilon_{pad} = 10}$ $\boxed{\varepsilon_{pad} = 50}$

R%"F5O:)%":

! 2-D Model of the EM problem related to MRI give sufficient physical insight into electro-magnetics of the problem

! New ideas/approaches can be quickly checked for usefulness

! here the cases ε_{pad} $\in$ {10, 50} have been investigated in detail

! the 90¡ sectorial pads can be used to improve the |B1+| profile along specific cut-planes

! but there are also cut -planes with deteriorate |B1+| profile

! the dielectric pads can be used to move the strong displacement currents into the pads

! ÒcurlyÓ (inhomogeneous) B1-field also inside pads

! different ÒregimesÓ depending on displacement current distribution can be defined